From Centrosymmetric $(C_4H_8N_5)(SbF_4)$ to Polar $(C_4H_7N_4O)(SbF_4)$: A New UV Nonlinear Optical Material Achieved by Functional Group Modulation

Zhi-Xiang Wang,[a,c] Chun-Li Hu,[a] Chuan-Fu Sun,*[b] Jiang-Gao Mao[a] and Fang Kong*[a,b]

a State Key Laboratory of Functional Crystals and devices, Fujian Institute of Research on the Structure of Matter, Chinese Academy of Sciences, Fuzhou 350002, P. R. China. E-mail: kongfang@fjirsm.ac.cn

b State Key Laboratory of Structural Chemistry, Fujian Institute of Research on the Structure of Matter, Chinese Academy of Sciences, Fuzhou 350002, P. R. China. E-mail: cfsun@fjirsm.ac.cn

c College of Chemistry, Fuzhou University, Fuzhou 350108. P. R. China.

E-mail: kongfang@fjirsm.ac.cn

Supporting Information

S1. Experimental Section

Reagents and Instruments

SbF_3 (Adamas-beta, 99.99%), HF (Adamas-beta, 30% in water), $C_5H_8N_4O$ (Adamas-beta, 99.99%) and $C_4H_7N_5$ (Adamas-beta, 99.99%) were obtained from commercial sources and used without further purification.

Powder X-ray diffraction (PXRD) patterns of $(C_4H_8N_5)(SbF_4)$ and $(C_4H_7N_4O)(SbF_4)$ were collected on the Miniflex 600 powder X-ray diffractometer using Cu Kα radiation (λ = 1.54186 Å) at room temperature in the angular range of 2θ = 5-70° with a scan step size of 0.02°.

IR spectra was carried out on a Magna 750 FT-IR spectrometer using air as background in the range of 4000–400 cm^{-1} with a resolution of 2 cm^{-1} at room temperature.

The UV-vis-NIR spectra was obtained at 2000–200 nm by a PerkinElmer Lambda 900 spectrophotometer using $BaSO_4$ as the reference, and the reflection spectra was converted into an absorption spectrum using the Kubelka-Munk function. Absorption data was calculated from the diffuse reflection data by the Kubelka-Munk function: $\alpha/S = (1-R)^2/2R$, where α and S represent the absorption coefficient and the scattering coefficient, respectively. The band gap value can be given by extrapolating the absorption edge to the baseline in the α/S vs. energy graph[1].

Thermogravimetric analyses (TGA) was measured by Netzsch STA 499C installation. The samples about 3.0-5.0 mg were placed in alumina crucibles and heated

in 20-800 °C at a rate of 15 K/min under N_2 atmosphere.

SHG Measurement. Powder SHG measurements were conducted using a modified method of Kurtz and Perry. Irradiation laser (λ = 1.064 μm) is generated by a Nd: YAG solid-state laser equipped with a Q switch. The $(C_4H_7N_4O)(SbF_4)$ pure crystal samples ground into powder were sieved according to seven different particle size ranges (25-45,45−53, 53-75, 75−105, 105−150 and 150−210 μm). KH_2PO_4 (KDP) samples in the same size range were also be prepared, which were used as reference. SHG signals oscilloscope traces of $(C_4H_7N_4O)(SbF_4)$ and KDP samples in the particle size range (150−210 μm) were recorded.

Syntheses

Antimony trifluoride SbF_3 (0.534g, 3mmol) and 6-methyl-1,3,5-triazine-2,4-diyldiamine $C_4H_7N_5$ (0.462g, 3mmol) were dissolved in 10 ml deionized water, 5 ml ethanol and 1 ml HF at room temperature. The mixture was allowed to evaporate slowly at room temperature and block-shaped colorless crystals of $(C_4H_8N_5)(SbF_4)$ were isolated in high yields of > 70% (based on $C_4H_5N_3$) after one week. When using 2-Amino-4-methoxy-6-methyl-1,3,5-triazine replace 6-methyl-1,3,5-triazine-2,4-diyldiamine, the molar ratio remains unchanged and the amount added is changed to 3mmol, following the same procedure and solvent to obtain the flaky colorless crystals of $(C_4H_7N_4O)(SbF_4)$ after one week, with the yield greater than 70% (based on $C_5H_8N_4O$). The purity of the crystals has been verified through X-ray diffraction (XRD) studies (Figure S3).

Single-crystal X-ray diffraction

Single crystal X-ray diffraction data of $(C_4H_8N_5)(SbF_4)$ and $(C_4H_7N_4O)(SbF_4)$ was obtained on Agilent Technologies SuperNova dual-wavelength CCD diffractometer with a graphite-monochromated Mo Kα radiation (λ = 0.71073 Å) at room temperature. Data reduction and cell refinement and were performed with *CrysAlisPro*. The structure was solved by the direct methods and refined by full-matrix least-squares fitting on F^2 using *Olex2-1.5* crystallographic software package[2, 3]. All of the atoms were refined with anisotropic thermal parameters and finally converged for $F_0^2 \geq 2\sigma(F_0^2)$. The structural data was also checked for possible missing symmetry with the program *PLATON*, and no higher symmetry was found[4, 5]. The detailed crystallographic data for $(C_4H_8N_5)(SbF_4)$ and $(C_4H_7N_4O)(SbF_4)$ was given in Table S1.

S2. Computational Method

Single-crystal structural data of $(C_4H_8N_5)(SbF_4)$ and $(C_4H_7N_4O)(SbF_4)$ was used for the theoretical calculations. The electronic structures were performed using a plane-wave basis set and pseudo-potentials within density functional theory (DFT) implemented in the total-energy code CASTEP[6]. For the exchange and correlation functional, we chose Perdew–Burke–Ernzerhof (PBE) in the generalized gradient approximation (GGA)[7]. The interactions between the ionic cores and the electrons were described by the ultrasoft pseudopotential[8]. The following valence-electron configurations were considered in the computation: C-$2s^12p^2$, H-$1s^1$, N-$2s^22p^3$, O-$2s^22p^4$, Sb-$5s^25p^3$ and F-$2s^22p^5$. The numbers of plane waves included in the basis sets were determined by cutoff energy of 850 eV for $(C_4H_8N_5)(SbF_4)$ and $(C_4H_7N_4O)(SbF_4)$. The numerical integration of the Brillouin zone was performed using Monkhorst-Pack k-point sampling of 5 × 3 × 3 for $(C_4H_8N_5)(SbF_4)$ and 2 × 5 × 3 for $(C_4H_7N_4O)(SbF_4)$. The other parameters and convergent criteria were the default values of CASTEP code.

Calculated method of linear optical response properties

The calculations of linear optical properties in terms of the complex dielectric function $\varepsilon(\omega) = \varepsilon_1(\omega) + i\varepsilon_2(\omega)$ were made. The imaginary part of the dielectric function ε2 was given in the following equation:

$$\varepsilon^{ij}_2(\omega) = \frac{8\pi^2h^2e^2}{(m^2V)}\sum_k\sum_{cv}(f_c - f_v)\frac{p^i_{cv}(k)p^j_{cv}(k)}{E^2_{vc}}\ \delta[E_c(k) - E_v(k) - h\omega]$$

The f_c and f_v represent the fermi distribution functions of the conduction and valence band. The term $p^i_{cv}(k)$ denotes the momentum matrix element transition from the energy level c of the conduction band to the level v of the valence band at the *k*th point in the

Brillouin zone (BZ), and *V* is the volume of the unit cell.

The real part $\varepsilon_1(\omega)$ of the dielectric function $\varepsilon(\omega)$ follows from the Kramer–Kronig relationship. All the other optical constants may be derived from $\varepsilon_1(\omega)$ and $\varepsilon_2(\omega)$. For example, the refractive index $n(\omega)$ can be calculated using the following expression[7]:

$$n(\omega)=\left(\frac{1}{\sqrt{2}}\right)\left[\sqrt{\varepsilon_1^2(\omega)+\varepsilon_2^2(\omega)}+\varepsilon_1(\omega)\right]^{1/2}$$

Calculated method of hyperpolarizability and anisotropy of organic molecules

Firstly, organic group models were established in Materials Studio. Next, the corresponding calculation methods and basis group were used to obtain the data in Gaussian. Finally, Multiwfn was used to analyze the output of hyperpolarizability and anisotropy.

Table S1. Summary of crystal data and structural refinements for $(C_4H_8N_5)(SbF_4)$ and $(C_4H_7N_4O)(SbF_4)$.

molecular formula	**$(C_4H_8N_5)(SbF_4)$**	**$(C_4H_7N_4O)(SbF_4)$**
Formula Weight	323.90	324.89
crystal system	triclinic	monoclinic
space group	*P*-1	*Pc*
Temperature(K)	294.21	100.15
F(000)	308.0	308
a/Å	5.0998(3)	11.4719(5)
b/Å	9.4607(5)	4.6982(2)
c/Å	10.3378(6)	9.1703(4)
α(deg)	68.330(5)	90
β(deg)	77.847(5)	113.104(5)
γ(deg)	85.276(5)	90
V/Å^3	453.13(5)	454.61(4)
Z	2	2
Dc(g.cm^{-3})	2.374	2.373
GOF on F^2	1.065	1.053
R_1, $wR_2[I > 2\sigma(I)]^a$	$R_1 = 0.0203$, $wR_2 = 0.0498$	$R_1 = 0.0170$, $wR_2 = 0.0395$
R_1, wR_2 (all data)^a	$R_1 = 0.0217$, $wR_2 = 0.0504$	$R_1 = 0.0171$, $wR_2 = 0.0396$

$^a R_1 = \sum||F_o| - |F_c||/\sum|F_o|$, $wR_2 = \{\sum w[(F_o)^2 - (F_c)^2]^2/\sum w[(F_o)^2]^2\}^{1/2}$

Table S2. Calculated bond valences for $(C_4H_8N_5)(SbF_4)$ and $(C_4H_7N_4O)(SbF_4)$.

Compound	Bond	Bond lengths	Bond-valence	BVS
$(C_4H_8N_5)(SbF_4)$	Sb(1)-F(1)	2.0646(16)	0.612	3.046
	Sb(1)-F(2)	1.9430(16)	0.850	
	Sb(1)-F(3)	2.0311(15)	0.670	
	Sb(1)-F(4)	1.9161(16)	0.914	
$(C_4H_7N_4O)(SbF_4)$	Sb(1)-F(1)	2.052(3)	0.633	2.987
	Sb(1)-F(2)	1.938(3)	0.861	
	Sb(1)-F(3)	2.068(3)	0.606	
	Sb(1)-F(4)	1.927(3)	0.887	

Symmetry transformations used to generate equivalent atoms:
#1 +X,1/2-Y,+Z; #2 +X,3/2-Y,+Z; #3 1-X,1-Y,-Z; #4 1-X,-1/2+Y,-Z; #5 1-X,1-Y,1-Z; #6 1-X,-1/2+Y,1-Z; #7 3/2-X,-1/2+Y,1/2+Z; #8 3/2-X,1-Y,1/2+Z;

Table S3. Hydrogen bond lengths (Å) and angles (°) for $(C_3H_7N_6)_2(SbF_5)\cdot H_2O$, $(C_4H_8N_5)(SbF_4)$ and $(C_4H_7N_4O)(SbF_4)$.

Compounds	D—H···A	d(D—H)	d(H···A)	d(D···A)	∠(D—H···A)
$(C_3H_7N_6)_2(SbF_5)\cdot H_2O$	O1—H2c···F2	0.85	2.04	2.872(4)	166.2
	O1—H1d···F4	0.85	2.05	2.886(4)	170.0
	N2—H2···F2	0.820(18)	1.915(19)	2.7160(10)	165(3)
	N3—H3a···F4	0.86	2.17	2.896(3)	142.2
	N3—H3b···F5	0.86	1.98	2.824(3)	168.0
	N7—H7b···F1	0.86	2.18	2.887(3)	139.3
	N8—H8···F1	0.839(19)	1.96(3)	2.738(3)	153(4)
	N9—H9b···O1	0.86	2.07	2.856(4)	151.9
$(C_4H_8N_5)(SbF_4)$	N2—H2a···F4	0.86	2.05	2.867(3)	158
	N2—H2b···N1	0.86	2.17	3.025(3)	176
	N4—H4a···F2	0.86	2.46	2.914(3)	114
	N4—H4a···F3	0.86	2.01	2.838(3)	162
	N4—H4b···F2	0.86	2.06	2.914(3)	175
	N5—H5…F1	0.86	1.76	2.616(3)	177
	C1—H1b…F4	0.96	2.36	3.251(3)	154
$(C_4H_7N_4O)(SbF_4)$	N1—H1···F3	0.77(6)	1.95(6)	2.698(6)	166(6)
	N2—H2···F1	0.84(7)	1.82(7)	2.647(6)	171(7)
	N4—H4a···F2	0.88	2.08	2.898(6)	154
	N4—H4b···F3	0.88	1.94	2.798(6)	166

Table S4. Comparison of the SHG efficiencies, optical band gap (> 4.20 eV), and birefringence among serval reported Sb-based NLO compounds.

Compounds	SHG effect	Band gap	Birefringence	Ref.
$K_2SO_4·SbF_3$	0.1 × KDP	4.44 eV	N/A	[9]
$Rb_2SO_4·(SbF_3)_2$	0.5 × KDP	4.69 eV	N/A	[10]
$NH_4SbF_2SO_4$	0.7 × KDP	4.67 eV	0.138@1064 nm^{calc}	[11]
$Sb_4O_4(SO_4)(OH)_2$	1.2 × KDP	4.41 eV	0.147@1064 nm^{calc}	[12]
$NH_4SbClSO_4$	1.7 × KDP	4.54 eV	N/A	[13]
$C(NH_2)_3SbF_4$	2.0 × KDP	4.80 eV	0.08@532 nm^{calc}	[14]
$(C_5H_7N_2)(Sb_2F_7)$	2.0 × KDP	4.51 eV	0.134@546 nm^{meas}	[15]
$Sb[CS(NH_2)_2]_2Br_3$	2.5 × KDP	5.17 eV	0.112@550 nm^{meas}	[16]
$CsSbF_2SO_4$	3.0 × KDP	4.76 eV	0.112@546 nm^{calc}	[17]
$NaSb_3F_{10}$	3.2 × KDP	5.00 eV	N/A	[18]
α-$2SbF_3·Gly$	3.3 × KDP	4.78 eV	0.146@546 nm^{calc}	[19]
$SbF_3·Gly$	3.6 × KDP	4.63 eV	0.057@1064 nm^{calc}	[20]
$K_2Sb(P_2O_7)F$	4.0 × KDP	4.74 eV	0.162@546 nm^{calc}	[21]
$(C_4H_7N_4O)(SbF_4)$	4.2 × KDP	4.40 eV	0.155@546 nm^{calc}	This work
$Rb_2Sb(P_2O_7)F$	5.1 × KDP	4.76 eV	0.15@546 nm^{meas}	[22]
$(C_5H_5NO)(Sb_2OF_4)$	12.0 × KDP	4.59 eV	0.513@546 nm^{meas}	[15]

Table S5. The assignments of the IR absorption peaks for $(C_4H_8N_5)(SbF_4)$ and $(C_4H_7N_4O)(SbF_4)$.

Assignment (cm^{-1})	$(C_4H_8N_5)(SbF_4)$	$(C_4H_7N_4O)(SbF_4)$
ν(N−H)	3358, 3143	3375,3183
ν(C−H)	1050-623	2932-2769, 1082-650
ν(C=O)	/	1760-1600
ν(C−N)	1383-1094	1308-1082
ν(Sb−F)	600-450	600-450

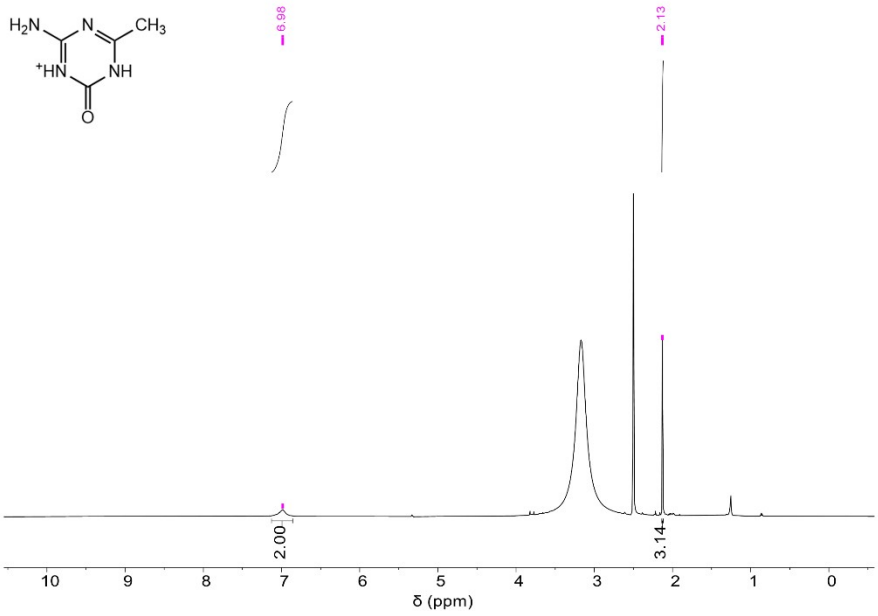

Figure S1. The ^{1}H NMR spectrum of the crystal $(C_4H_7N_4O)(SbF_4)$.

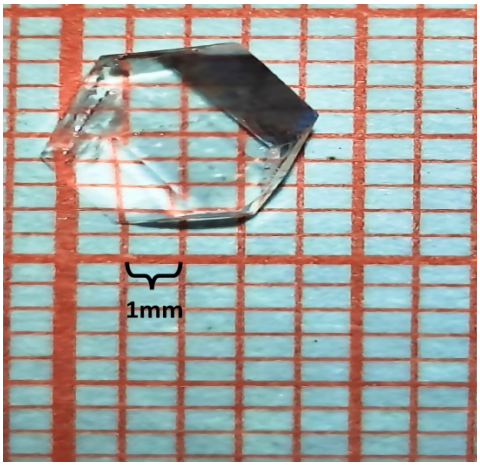

(a)

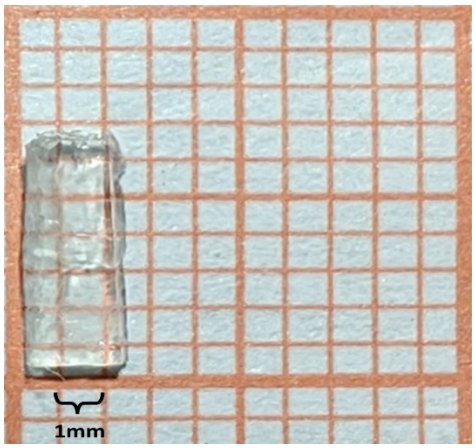

(b)

Figure S2. The pictures of crystal $(C_4H_8N_5)(SbF_4)$ (8×4×2 mm^3) (a) and crystal $(C_4H_7N_4O)(SbF_4)$ (7×2×1 mm^3) (b).

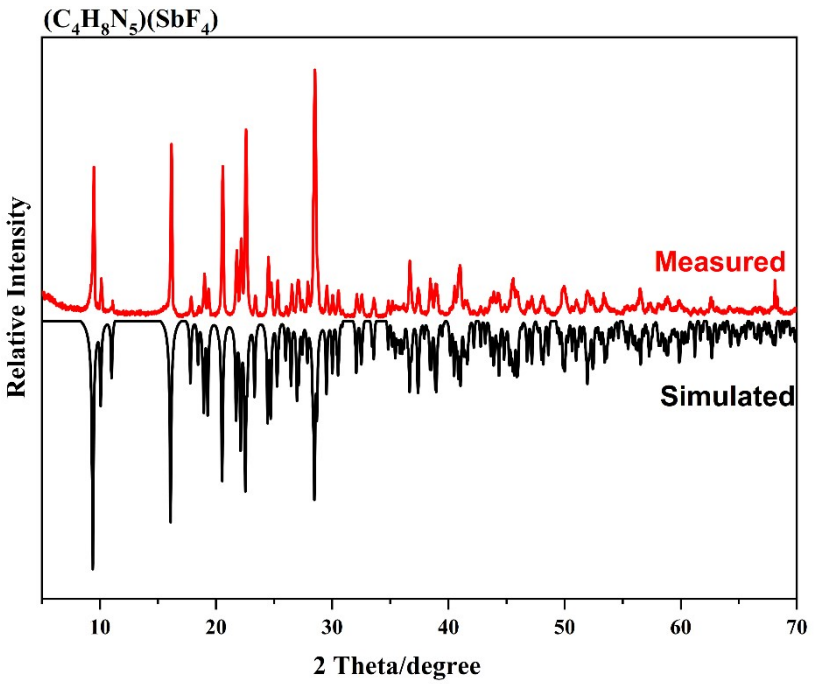

(a)

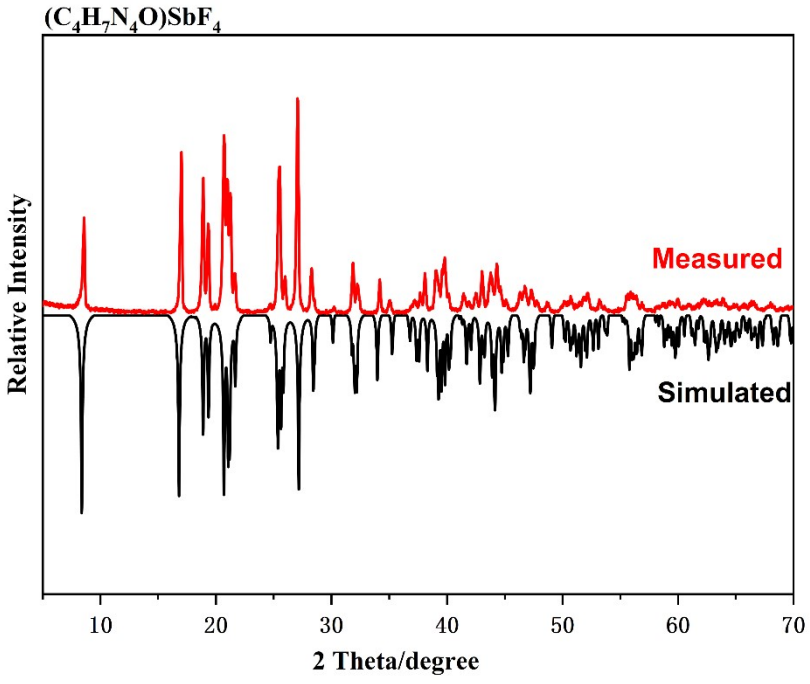

(b)

Figure S3. Simulated and measured powder X-ray diffraction patterns of $(C_4H_8N_5)(SbF_4)$ (a) and $(C_4H_7N_4O)(SbF_4)$ (b).

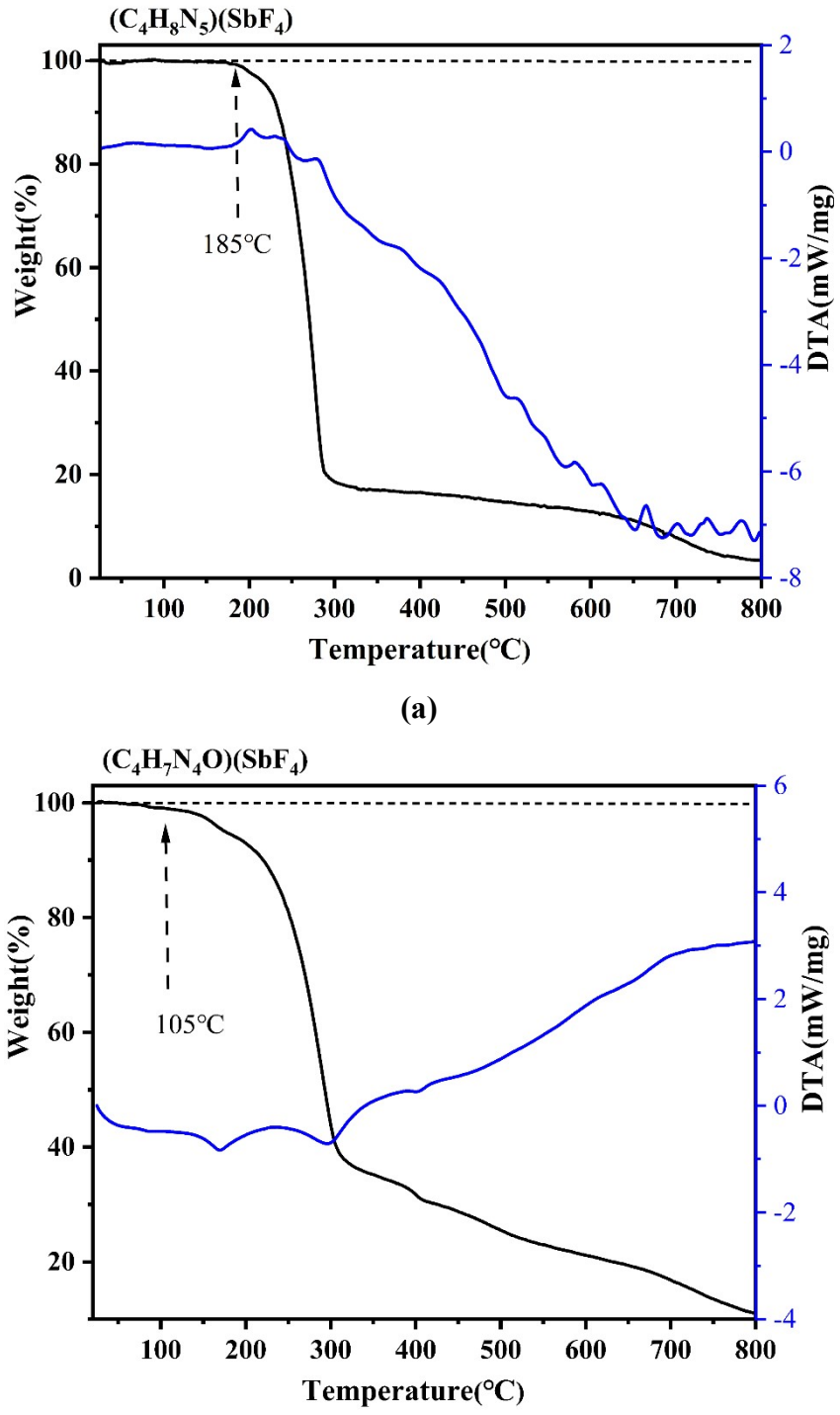

Figure S4. The TGA results of $(C_4H_8N_5)(SbF_4)$ (a) and $(C_4H_7N_4O)(SbF_4)$ (b)

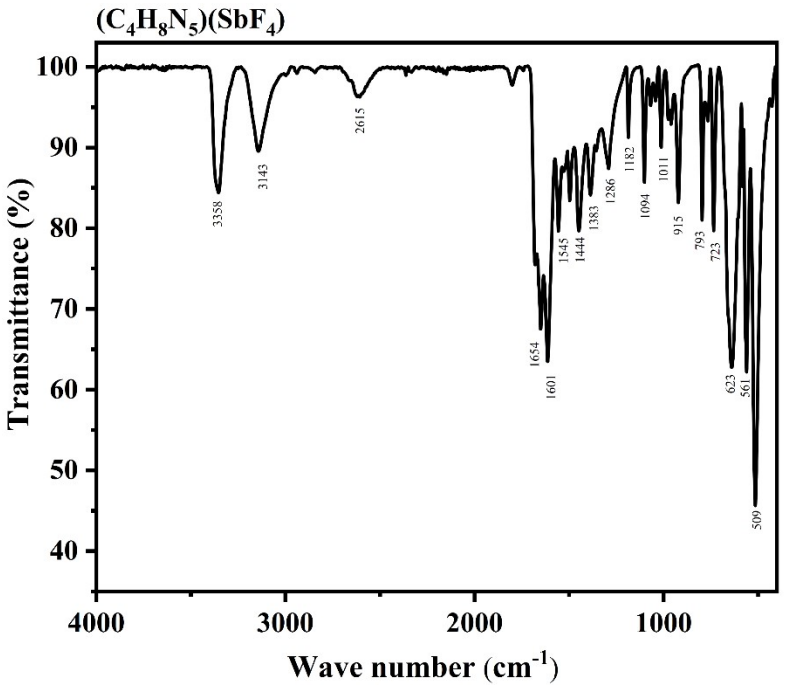

(a)

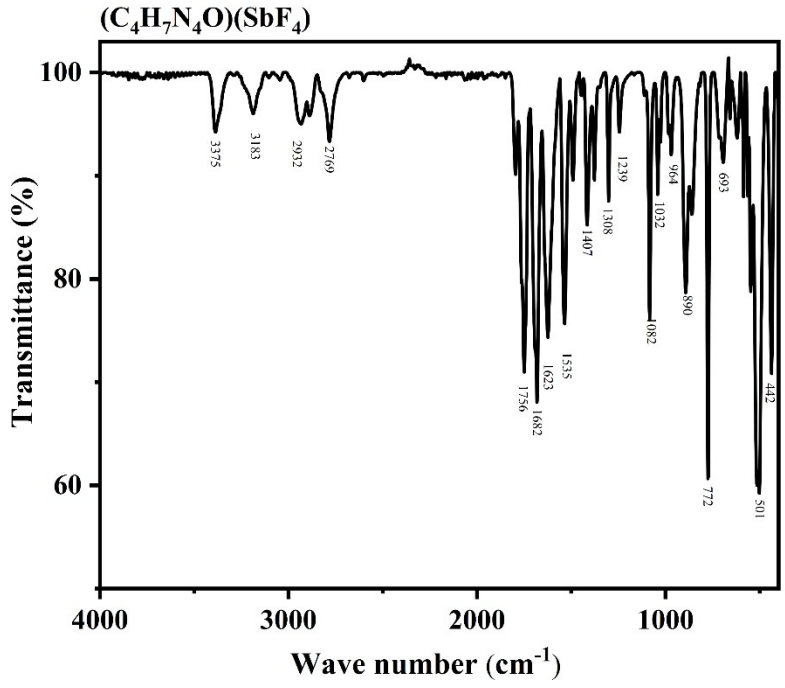

(b)

Figure S5. IR spectrum of $(C_4H_8N_5)(SbF_4)$ (a) and $(C_4H_7N_4O)(SbF_4)$ (b).

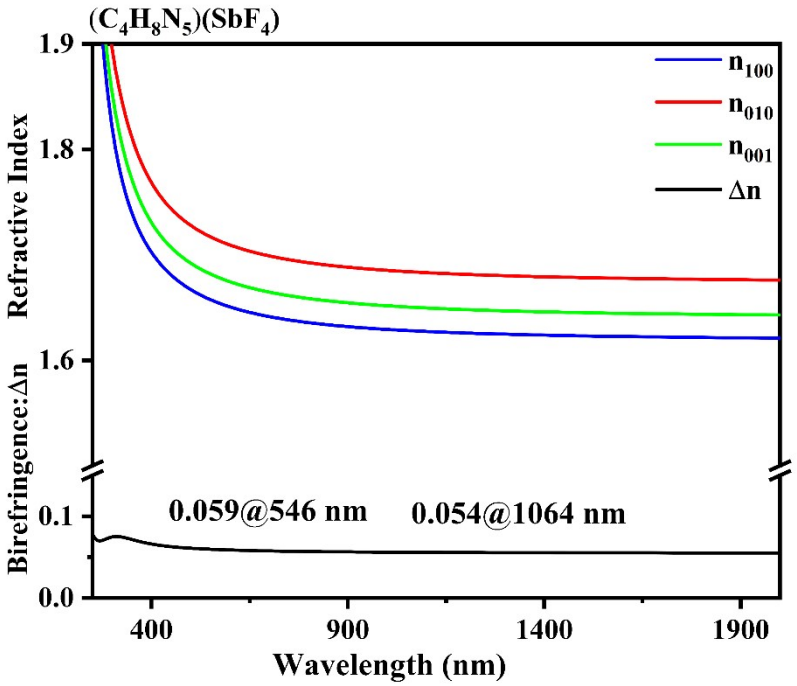

Figure S6. The calculated birefringence curves of $(C_4H_8N_5)(SbF_4)$.

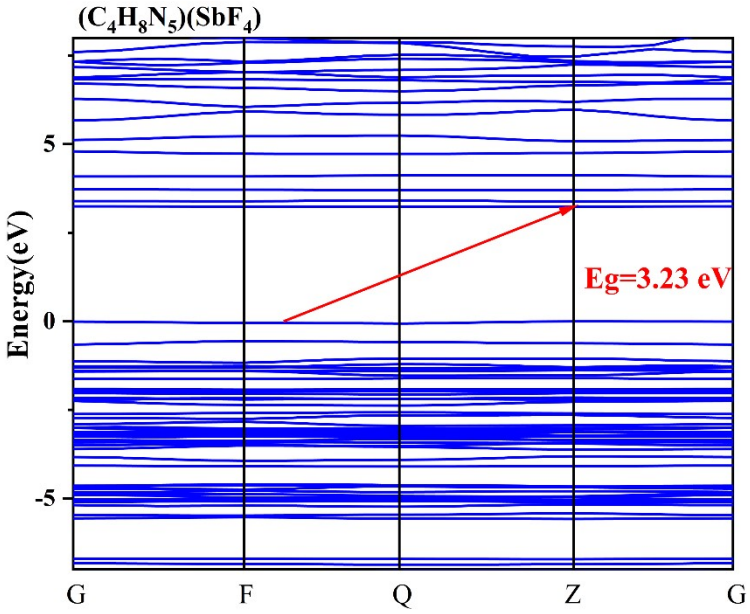

(a)

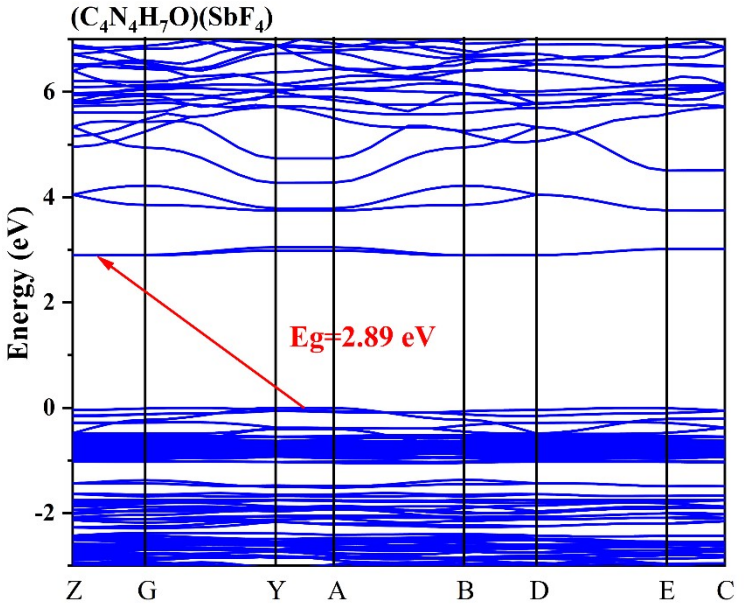

(b)

Figure S7. Calculated band structures of $(C_4H_8N_5)(SbF_4)$ (a) and $(C_4H_7N_4O)(SbF_4)$ (b).

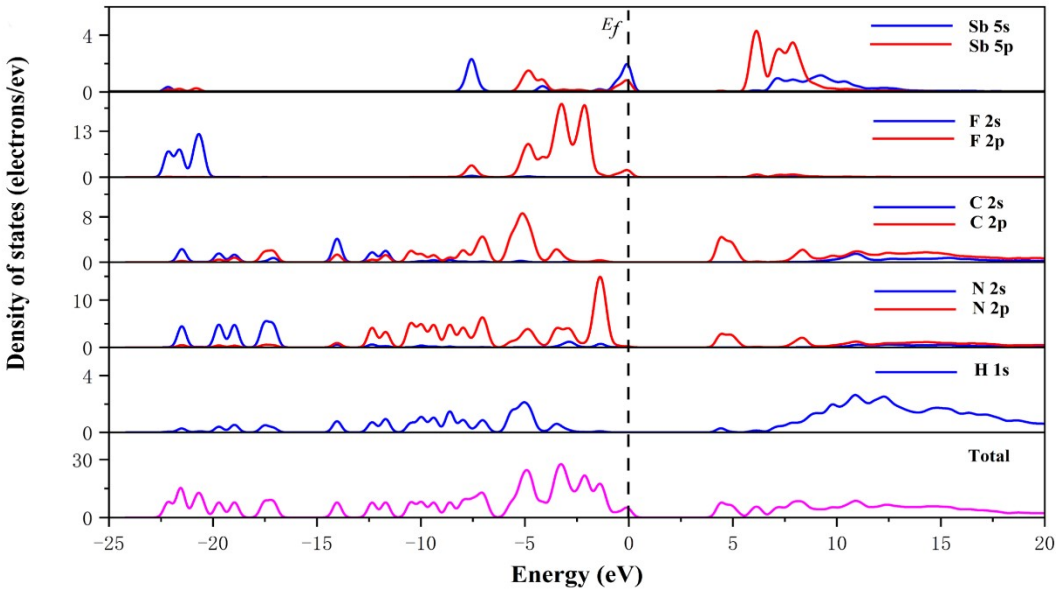

Figure S8. The total and partial density of states of $(C_4H_8N_5)(SbF_4)$.

References

[1] P. Kubelka and F. Munk, *Technol. Physical* 1931, **12**, 259−274.

[2] G. M. Sheldrick, *Acta Cryst*., 2015, **C71**, 3-8.

[3] O. V. Dolomanov, L. J. Bourhis, R. J. Gildea, J. A. K. Howard and H. Puschmann, *J. Appl. Cryst.*, 2009, **42**, 339-341.

[4] R. H. Blessing, *Acta Cryst*., 1995, **A51**, 33−38.

[5] A. L. Spek, *J. Appl. Cryst.*, 2003, **36**, 7−13.

[6] M. D. Segall, P. J. D. Lindan, M. J. Probert, C. J. Pickard, P. J. Hasnip, S. J. Clark and M. C. Payne, *Phys-Condens Mat*., 2002, **14**, 2717-2744.

[7] V. Milman, B. Winkler, J. A. White, C. J. Pickard, M. C. Payne, E. V. Akhmatskaya and R. H. Nobes, *Int. J. Quantum. Chem.*, 2000, **77**, 895-910.

[8] J. P. Perdew, K. Burke and M. Ernzerhof, *Phys. Rev. Lett.*, 1996, **77**, 3865-3868.

[9] F. He, L. Wang, C. Hu, J. Zhou, Q. Li, L. Huang, D. Gao, J. Bi, X. Wang and G. Zou, *Dalton Trans*, 2018, **47**, 17486-17492.

[10] Q. Wang, L. Wang, X. Zhao, L. Huang, D. Gao, J. Bi, X. Wang and G. Zou, *Inorg. Chem. Front.*, 2019, **6**, 3125-3132.

[11] F. He, Y. Ge, X. Zhao, J. He, L. Huang, D. Gao, J. Bi, X. Wang and G. Zou, *Dalton Trans*, 2020, **49**, 5276-5282.

[12] Q. Wei, K. Wang, C. He, L. Wei, X.-F. Li, S. Zhang, X.-T. An, J.-H. Li and G.-M. Wang, *Inorg. Chem*., 2021, **60**, 11648-11654.

[13] F. He, Y. Ge, X. Zhao, J. He, L. Huang, D. Gao, J. Bi, X. Wang and G. Zou, *Dalton Trans*, 2020, **49**, 5276-5282.

[14] M. Zhang, B. Zhang, D. Yang and Y. Wang, *Inorg. Chem.*, 2021, **60**, 18483-18489.

[15] L. Qi, X. Jiang, K. Duanmu, C. Wu, Z. Lin, Z. Huang, M. G. Humphrey and C. Zhang, *J. Am. Chem. Soc.*, 2024, **146**, 9975-9983.

[16] Karthick N, Sankar R, Jayavel R, *J. Cryst. Growth*, 2009, **312(1)**, 114–119.

[17] X. Dong, L. Huang, C. Hu, H. Zeng, Z. Lin, X. Wang, K. M. Ok and G. Zou, *Angew. Chem. Int. Edit.*, 2019, **58**, 6528-6534.

[18] G. Zhang, J. Qin, T. Liu, Y. Li, Y. Wu and C. Chen, *Appl. Phys. Lett.*, 2009, **95**, 261104.

[19] Y. Kuk, Z. Bai, Y. Li and K. M. Ok, *Chem. Mat.*, 2025, **37**, 1306-1313.

[20] Z. Bai, J. Lee, C.-L. Hu, G. Zou and K. M. Ok, *Chem. Sci.*, 2024, **15**, 6572-6576.

[21] S. V. Krivovichev and L. Bindi, *Angew. Chem. Int. Edit*., 2020, **60**, 3854-3855.

[22] X. Dong, H. Huang, L. Huang, Y. Zhou, B. Zhang, H. Zeng, Z. Lin and G. Zou, *Angew. Chem. Int. Edit*, 2024, **63**, e202318976.